RESEARCH ARTICLE

SAMRIDDHI Volume 15, Issue 3, 2023 Print ISSN: 2229-7111 Online ISSN: 2454-5767

A Comparative Study of Conventional Transition Model and Reverse Transition Model for Wireless and Radar Applications

Atul Varshney*, Vipul Sharma

Department of Electronics and Communication, Gurukula Kangri (Deemed to be University) Haridwar, Uttarakhand, India

Abstract

Microstrip line-to-waveguide transitions (MLWT) finds various applications in the field of RADAR engineering, navigation science, medical electronics, household equipment, satellite tracking equipment, wireless communications etc. Conventionally, the MLWT is designed so that the microstrip line is inserted in E-plane and perpendicular to the waveguide's side wall, while the microstrip probe's radiating face is towards the waveguide's open end port. In this paper, an MLWT has been designed for Ka-band applications and the transition has been designed in such a way that the radiating face of the inserted microstrip line probe is towards the short circuit end of the waveguide. The method is called the reverse transition method. The microstrip signal reflected from the short circuit end comes in additive phase with the traveling wave and the strength of the traveling wave increases. MLWT has been developed using this method and results for Ka-band applications are presented in this paper. This work reported more than 20 dB improvement in return loss (RL), 0.1dB improvement in insertion loss (IL) and almost 7 to 8% enhancement in 10dB fractional bandwidth compared to the conventional method. Comparative analysis of the two methods has been shown in tabular form at the end of the paper.

Keywords: Electrical equivalent circuit, Ka-band, Microstrip line, reverse transition, transition,WR-28.

SAMRIDDHI : A Journal of Physical Sciences, Engineering and Technology (2023); DOI: 10.18090/samriddhi.v15i03.11

Introduction

In the recent trends, many transitions are available, and further research are carried on for microwave upper bands, millimeter and sub-millimeter wave frequency range for future wireless, satellite, defense and RADAR applications to provide compatible connections to planar MMIC/MIC microstrip circuits, transmitter/receiver sections with antennas.[1] A reverse transition (RT) is an alternative methodology of exciting transverse electric dominant mode TE_{10} into the rectangular waveguide by extending a portion of the microstrip line main strip conductor or patch.[2] E.R. Murphy first coined the idea in 1984,[3] but afterward, no substantial research has been reported till date. The RT has only one difference of inserting a microrstrip (MS) line facing the conventional transition in design, although all the materials and rest parameters are constants. Nevertheless, it is essential to design RT at the same centre frequency of conventional transition because of its results performance is far better than to the conventional one in terms of their return loss (RL), insertion loss (IL) and fractional bandwidth (BW) of interest.

This paper explains the tabular, parameters-based comparison between RT and conventional transitions. With this improved performance, the RT could be the best option to use into the MIMO/Massive MIMO array antenna systems, WiMAX, planar circuits interconnect with MIC and MMICs.

Corresponding Author: Atul Varshney, Department of Electronics and Communication, Gurukula Kangri (Deemed to be University) Haridwar, Uttarakhand, India, e-mail: atulgkvright@gmail.com

How to cite this article: Varshney, A., Sharma, V. (2023). A Comparative Study of Conventional Transition Model and Reverse Transition Model for Wireless and Radar Applications. *SAMRIDDHI : A Journal of Physical Sciences, Engineering and Technology,* 15(3), 346-353.

Source of support: Nil

Conflict of interest: None

Literature Review

Nowadays, electromagnetic energy transmission amongst transmission lines of different geometries is required. This could be achieved through power combiners or launchers. In other words, we can say that the electromagnetic energy is coupled between two dissimilar transmission lines by means of transitions. For this purpose, a huge number of MS line-to-RWG transitions are developed and existing.[1] A huge number of in-line [2-10] and side inserted 90° MS line-to-RWG transition [3,11-29] at various microwave band by inserting a portion of MS line into the rectangular waveguide (RWG) with different impedance matching and field matching

methodologies have been already designed, and research is being carryon on these designs for the betterment of RL, IL, fractional BW, VSWR etc. [11-13] R. Gupta and P. P. Kumar demonstrate a right-angled Ka-band waveguide to coaxial line transition, which impedance and field matching are achieved through coaxial probe and ridge waveguide for space-borne and military electronic systems. [29] A conventional in-line end-inserted Ka-band integrated microstrip and waveguide in planar form has been designed and realized by Dominic Deslandes and Ke Wu. It has better RL and IL but poor BW. [5] Cun Long, Li, *et al.* designed a low-cost prototype, single-layer PCB, compact structure and easy integration, wideband conventional transition for millimeter wave applications.[10] Several researchers have designed a conventional E-plane 90° microstrip to rectangular waveguide transitions for Ka-band by using different technologies for impedance and field matching like a stepped transformer, Chebyshev transformer, bow tie techniques, semicircular ring patch, complementary SRR etc. [11,14,15,19,23,29,30] Earl R. Murphy patents his designed microstrip to waveguide transition based on conventional as well as on reverse insertion of microstrip into the waveguide. [12]

In this proposed work a reverse transition has been designed along with the conventional transition and all possible comparisons have been made in a well-arranged manner.

MS Line-to-RWG Transition Models

Two MS line-to-RWG transition design (one normally Conventional and other reverse transition) models have been designed, simulated using HFSS software and then compared in tabular format, keeping all design dimensions, parameters and material constant except that the MS line facing towards RWG port in Conventional case whereas it facing towards back short in case of reverse transition.

Design Parameters and Dimensions

All optimized common performance parameters for both conventional and reverse MS line-to-RWG transitions are given in Table 1. All dimensions are measured in mm.

Common Microstrip line

The inserted microstrip line in the RWG WR-28 to launch electromagnetic energy is common for both the Conventional and reverse transition models. MS line has three microstrips at MS port to excite electromagnetic energy, a second quarter wave transformer in the middle to match the dissimilar impedances of MS line and RWG for transverse electric dominant mode and the last section consists of a microstrip patch with two small circular patches at its base to maximize the coupling between the two transmission lines as shown in Figure 1.

Conventional MS Line-to-RWG Transition Model

Conventional transition design parameters are calculated using the design formulas [31] and then optimized as shown in Figure 3(a). Figure 3(b) represents the simulated return loss (RL) and insertion loss (IL) values of Conventional transition. The complex S-parameters values are present in Figure 3(c) obtained using

Table 1: Optimized common performance parameters of conventional and reverse transition models

Part name	*Designation*	*Parametric Values*
Rectangular Waveguide	Waveguide type	WR-28
	Dielectric	Air filled
	Broad side	a=7.112
	Narrow side	b= 3.556
	Waveguide length	LWG≈3*(λg/4) =21.4
Microstrip Line	Material	LWG (Cu)
	Width	Wstrip=0.37
	Length	Wstrip=7.244
	Thickness	t= .05
Quarter Wave Transformer	Material	Copper (Cu)
	Width	W λg/4 =0.24
	Length	L λg/4 =3.4
	Thickness	t = 0.05
Microstrip Rectangular Patch	Material	Copper (Cu)
	Width	WPatch =0.40
	Length	LPatch =1.556
	Thickness	t= .05
2-Patch Circles	Each base circle radius	r= 0.2
E-plane 90° broad side a, Slot	Dielectric	Air filled
	Width	WSlot =3.8
	Length	LSlot =1.48
	Height	HSlot =0.32
Ground	Material	Copper (Cu)
	Width	WGnd. =3.8
	Length	LGnd. =9.164
	Thickness	t= .05
Substrate	Material	Roger RT Duroid 5880 (tm)
	Width	WSub. =3.8
	Length	LSub. =14.2
	Height	h=0.127
Back Short	Back short distance	d =λg/4c = 3.4
	Broad side	a=7.112
	Narrow side	b=3.556

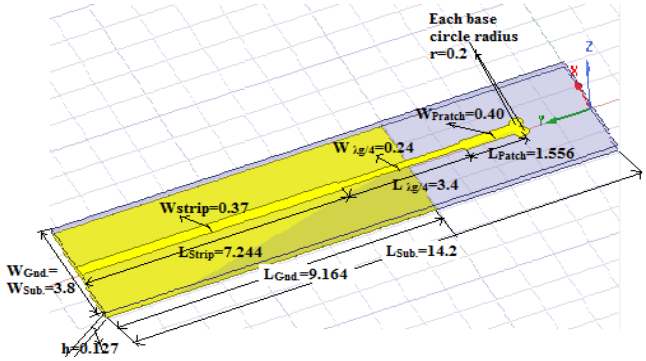

Figure 1: Common MS line for both Conventional and reverse transitions

HFSS at 30 GHz. These S-Parameters are used to find out RLC electrical equivalent circuits of conventional MS line-to-RWG transition (using conversion formulas [13]) by following the steps

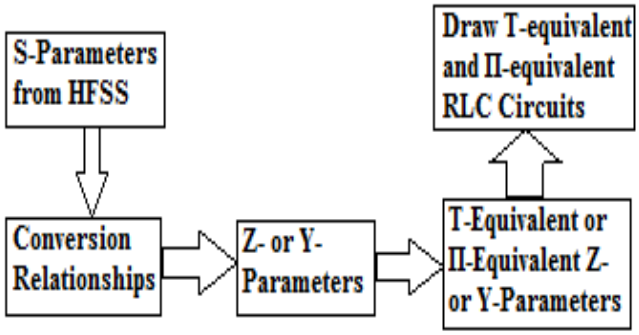

Figure 2: A Block diagram of RLC electrical equivalent circuits generation

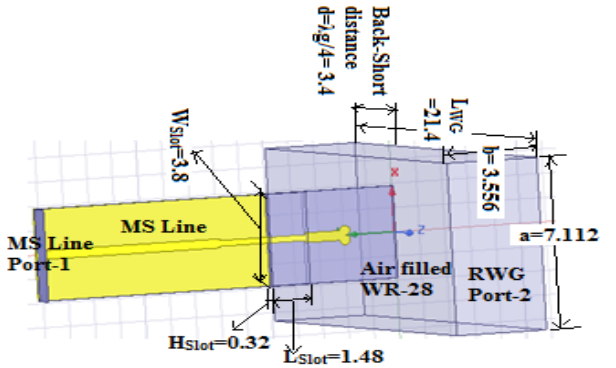

(a)

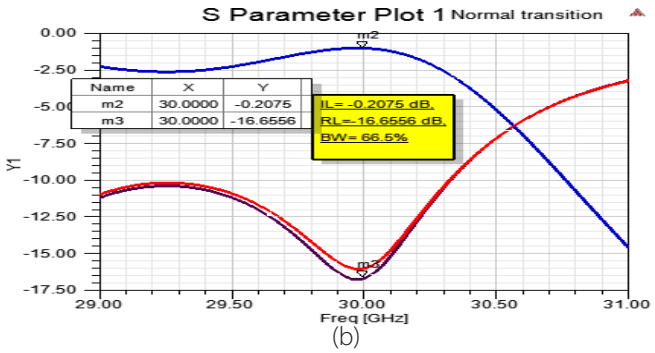

(b)

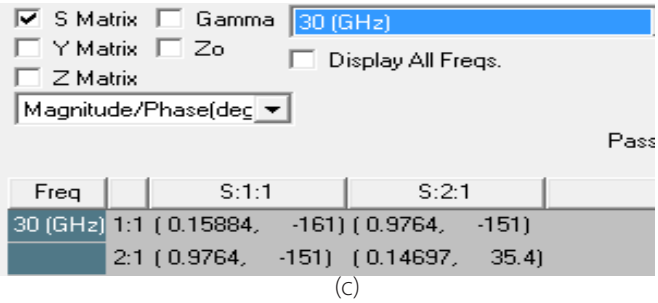

(c)

Figure 3: (a) Conventional MS line-to-RWG transition, (b) Simulated RL and IL of Conventional MS line-to-RWG, Transition, (c) S-Parameters of Conventional MS line-to-RWG Transition from HFSS

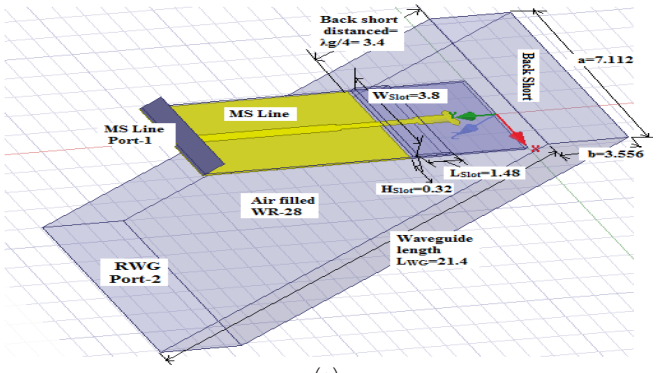

(a)

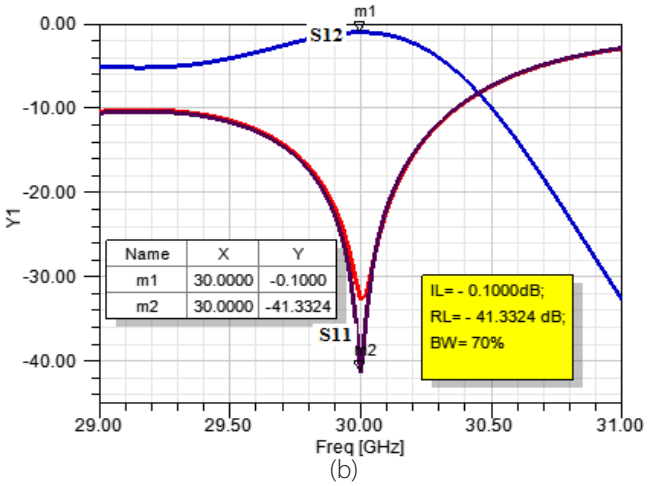

(b)

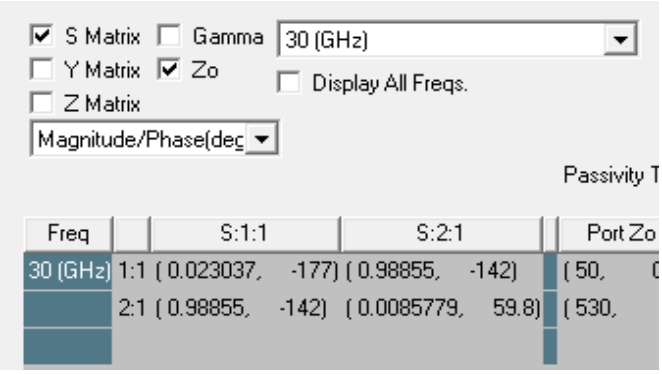

(c)

Figure 4: (a) Reverse MS line-to-RWG transition, (b) Simulated S-Parameters of RL and IL of Reverse Transition, (c) S-Parameters of Reverse MS line-to-RWG Transition from HFSS

mentioned in the below block diagram of Figure 2.

Reverse MS Line-to-RWG Transition Model

A reverse transition is designed with the same optimized parameters, materials and dimensions as provided in Table 1 for the Conventional transition to check out the hypothesis that reverse transition has unequal performance than Conventional transition. The reverse transition design, simulated return loss (RL) and, insertion loss (IL) and their

complex S-Parameter results are shown in Figure 4(a-c), respectively.

RLC Electrical Equivalent Circuits

RLC Electrical Equivalent Circuits of Conventional Transitions

The RLC electrical equivalent circuits (T-equivalent and Π-equivalent) of Conventional MS line-to-RWG transition are shown in Figures 5(a) and (b), respectively. The RLC component values are highlighted in Tables 4 and 5, respectively.

RLC Electrical Equivalent Circuits of Reverse Transitions

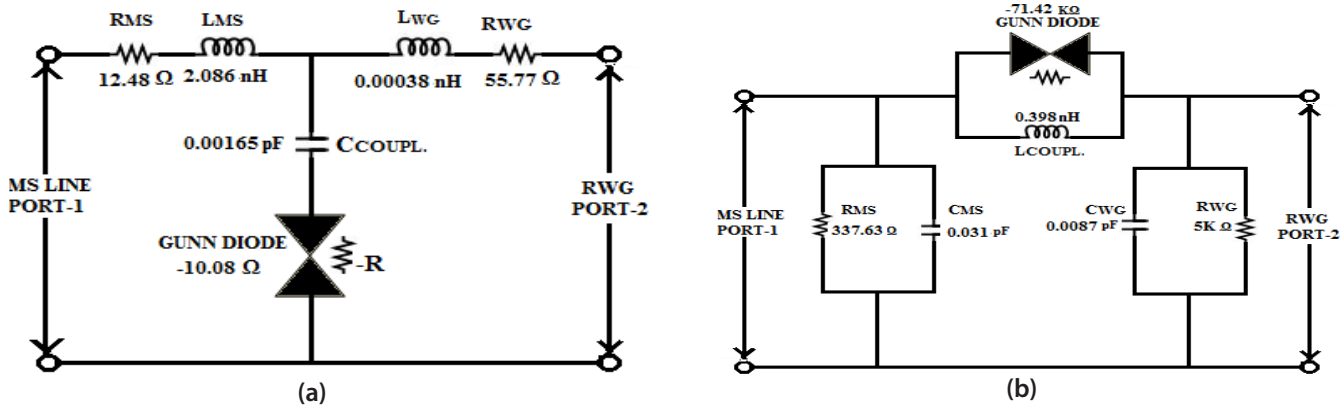

Figure 5: Ka-band Conventional MS line-to-RWG transition (a) Electrical T-equivalent circuit, (b) Electrical π-equivalent circuit

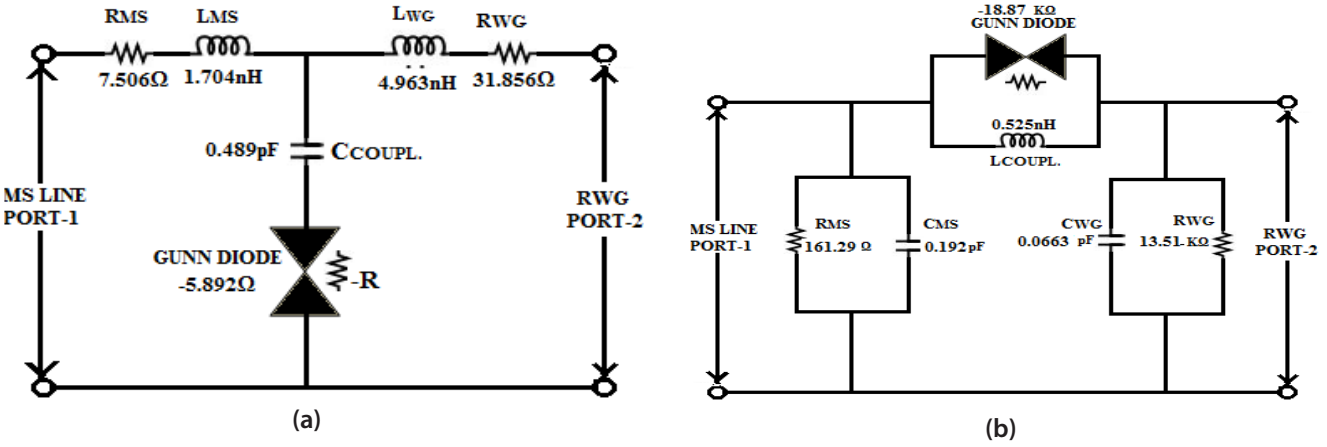

Figure 6: Ka-band MS line-to-RWG transition (a) Electrical T-equivalent circuit, (b)Electrical π-equivalent circuit

Table 2: Electrical T-Equivalent circuit elements

T-Equivalent	*MS Line*		*RWG*		*Coupling*	
Impedances	R_{MS}	L_{MS}	R_{WG}	C_{WG}	$C_{coup.}$	*Gunn Diode*
(in Ω)	(Ω)	(nH)	(Ω)	(pF)	(pF)	(-R) (Ω)
Z_A=12.48+ j393.20	12.48	2.086	…..	…..	…..	…..
Z_B=–10.08 – j320.88	…..	…..	…..	…..	0.00165	10.08
Z_C=55.77 – j1410.92	…..	…..	55.77	0.00038	…..	…..

Table 3: Electrical π-equivalent circuit elements

Π –Equivalent Admittances (in mho)	*MS Line*		*RWG*		*Coupling*	
	R_{MS} *(Ω)*	C_{MS} *(pF)*	R_{WG} *(Ω)*	C_{WG} *(pF)*	$L_{coup.}$ *(nH)*	*Gunn Diode (-R) (Ω)*
Y_A=0.001086 + j0.058	537.63	0.031	----	----	----	----
Y_B=– 0.00014 – j 0.0133	----	----	----	----	0.398	71.42K
Y_C=0.0002 + j 0.0163	----	----	5K	0.0087	----	----

Table 4: Electrical T-equivalent circuit elements

T-Equivalent Impedances (in Ω)	*MS Line*		*RWG*		*Coupling*	
	R_{MS} *(Ω)*	L_{MS} *(nH)*	R_{WG} *(Ω)*	L_{WG} *(nH)*	$C_{coup.}$ *(pF)*	*Gunn Diode (-R) (Ω)*
Z_A=7.506 + j 321.28	7.506	1.704	…..	…..	…..	…..
Z_B=–5.892 – j259.66	…..	…..	…..	…..	0.489	5.892
Z_C=31.856+ j935.50	…..	…..	31.856	4.963	…..	…..

Table 5: Electrical Π-Equivalent Circuit Elements

Π –Equivalent Admittances (in mho)	*MS Line*		*RWG*		*Coupling*	
	R_{MS} *(Ω)*	C_{MS} *(pF)*	R_{WG} *(Ω)*	C_{WG} *(pF)*	$L_{coup.}$ *(nH)*	*Gunn Diode (-R) (Ω)*
Y_A=0.00062 + j 0.0363	161.29	0.192	----	----	----	----
Y_B= -0.000053 – j 0.0101	----	----	----	----	0.525	18.87K
Y_C=0.000074+ j 0.0125	----	----	13.51K	0.0663	----	----

Table 6: Conventional Transition vs Reverse Transition model

S. No.	*Parameters*	*Conventional MS Line-to-RWG Transition*	*Reverse MS Line-to-RWG Transition*	*Comment*
1	Design Frequency	30 GHz	30 GHz	Same
2	Microstrip Face	Facing towards RWG Port-1	Facing towards RWG back-short	Opposite facing
3	Design Dimensions	AS shown in Table-I	AS shown in Table-I	All materials and dimensions are constant
4	Design	As shown in Figure 3(a)	As shown in Figure 4(a)	Same except that MS Line facing towards back short instead of waveguide port in reverse transition
5	Simulated Results	As shown in Figure 3(b)	As shown in Figure 4(b)	Improves by two times

6	Insertion loss (IL)	-0.2075dB	-0.1000 dB	Better in reverse transition
7	Return Loss (RL)	-16.6556 dB	-41.3324 dB	Greatly improves in reverse transition
8	10 dB Fractional Bandwidth (BW)	66.50%	72%	Enhanced by 7 to 8%
9	VSWR	1.355	1.031	VSWR improves
10	S-Parameter $[S]=\begin{bmatrix}S11 & S12\\ S21 & S22\end{bmatrix}$	$\begin{bmatrix}0.15884\angle-161^\circ & 0.9764\angle-151^\circ\\ 0.9764\angle-151^\circ & 0.14697\angle35.4^\circ\end{bmatrix}$	$\begin{bmatrix}0.02304\angle-177^\circ & 0.9885\angle-142^\circ\\ 0.9885\angle-142^\circ & 0.0086\angle59.8^\circ\end{bmatrix}$	All are complex quantity
11	Z-Parameters $[Z]=\begin{bmatrix}Z11 & Z12\\ Z21 & Z22\end{bmatrix}$	$\begin{bmatrix}72.363\angle88.1^\circ & 321.04\angle-91.8^\circ\\ 321.04\angle-91.8^\circ & 1091\angle87.6^\circ\end{bmatrix}$	$\begin{bmatrix}61.639\angle88.5^\circ & 259.73\angle-91.3^\circ\\ 259.73\angle-91.3^\circ & 676.34\angle87.8^\circ\end{bmatrix}$	All are complex quantity
12	Y-Parameters $[Y]=\begin{bmatrix}Y11 & Y12\\ Y21 & Y22\end{bmatrix}$	$\begin{bmatrix}0.0452\angle88.8^\circ & 0.0133\angle89.4^\circ\\ 0.0133\angle89.4^\circ & 0.003\angle89.3^\circ\end{bmatrix}$	$\begin{bmatrix}0.0262\angle88.8^\circ & 0.0101\angle89.6^\circ\\ 0.0101\angle89.6^\circ & 0.0024\angle89.5^\circ\end{bmatrix}$	All are complex quantity
13	T-Network Parameters (in Ω)	ZA = Z11–Z12=(12.48+ j393.20) ZB = Z12=(–10.08 – j320.88) ZC = Z22–Z12=(55.77 – j1410.92)	ZA = Z11–Z12 = (7.506 + j 321.28) ZB = Z12= (–5.892 – j259.66) ZC = Z22– Z12=(31.856+j935.50)	All are complex quantity
14	Π-Network Parameters (in mho)	YA= Y11+Y12=(0.001086+ j0.058) YB= –Y12=(– 0.00014 – j 0.0133) YC =Y22+Y12=(0.0002+ j 0.0163)	YA= Y11+Y12= (0.00062+ j 0.0363) YB= –Y12= (– 0.000053 – j 0.0101) YC =Y22+Y12= (0.000074+ j 0.0125)	All are complex quantity
15	Electrical T-Equivalent RLC Circuit	As shown in Figure 5(a)	As shown in Figure 6(a)	. The circuits are passive within the specified tolerance at all frequencies. .The circuits are same with little variations in their R, L and C values.
16	Electrical Π-Equivalent RLC Circuit	As shown in Figure 5(b)	As shown in Figure 6(b)	. The circuit is passive within the specified tolerance at all frequencies. .The circuits are same with little variations in their R, Land C values.

The RLC electrical equivalent circuits (T-equivalent and Π-equivalent) of reverse MS line-to-RWG transition are shown in Figure 6(a) and Figure 6(b), respectively. The RLC component values are highlighted in Tables 2 and 3, respectively.

Conventional transition vs Reverse Transition model

The comparison of the conventional MS line-to-RWG transition with the reverse MS line-to-RWG transition have been present in the tabular form in Table 6 in terms of all possible related parameters as shown in column two of the parameter. This table and a comment have been added on each comparison.

Results

Reverse MS line-to-RWG transition is an alternative way to couple microstrip line electromagnetic energy into the rectangular waveguide. It provides much better impedance matching in comparison to Conventional MS line interconnect. By keeping all materials, parameters and dimensions constants, the RL loss improves by a great extent and IL improves to 0.100 dB that of 0.2075 dB in Conventional transition. -10dB fractional bandwidth also increases by 7 to 8%. Both the transitions have the exactly same equivalent circuits with little variations in their R, L and C values. The negative resistance is represented by Gunn diode. The RLC Electrical equivalent circuits are passive in nature at all designed frequencies with

slight changes in their parameter values.

Conclusions

The reverse MS line-to-RWG transition is a better choice over the Conventional microstrip transition for microwave, RADAR, wireless and satellite communication applications to connect planar MMIC/MIC circuits with the waveguide sections and antenna transmitters and receivers. This article gives the general idea how to develop a reverse transition from a conventional one and vice-versa. A reverse transition has been developed for Ka-band applications and excellent performance has been reported as compared to conventional transition. The reverse transition has many peculiar advantages over Conventional transition like better IL, RL, VSWR, and bandwidth.

Recommendation

The novel simplified approach is not only limited to MS line interconnects nevertheless, possibly in future this technique may also be applicable to obtain reverse transition models of other existing microwave components such as slot line to RWG transition, RWG to circular waveguide transitions etc. The electrical equivalent of microstrip line interconnects are commonly used in modern mobile devices such as smartphones.

Acknowledgment

The authors would like to thank the Vice-chancellor, Dean FET and Head of the Department of Electronics and Communication as well as Microwave LAB and their supporting staff, FET, Gurukula Kangri Deemed to be University, Haridwar, India for providing the simulation environment of Ansoft HFSS and the measurement instruments.

References

[1] Varshney, A., & Sharma, V. (2020). A Comparative Study of Microwave Rectangular Waveguide-to-Microstrip Line Transition for Millimeterwave, Wireless Communications and Radar Applications. Microwave Review. 26 (2), 21-37.

[2] Hassan, S. E., Berggren, M., Scheiner, B., Michler, F., Weigel, R., & Lurz, F. (2019). Design of Planar Microstrip-to-Waveguide Transitions Using Topology Optimization. IEEE Radio and Wireless Symposium (RWS), Orlando, FL, USA, 1-3.

[3] Ren, Y., Li, K., Wang, F., Gao, B., & Wu, H. (2019). A Broadband Magnetic Coupling Microstrip to Waveguide Transition Using Complementary Split Ring Resonators. IEEE Access, 7, 17347-17353.

[4] Huang, X., & Wu, K.-L. (2012). A Broadband U-slot Coupled Microstrip-to-Waveguide Transition. IEEE Trans. Microw. Theory Techn., 60 (5), 1210-1217.

[5] Deslandes, D., & Wu, K. (2001). Integrated Microstrip and Rectangular Waveguide in Planar Form. IEEE Microwave and Wireless Components Letters, 11 (2), 68-70.

[6] Pérez-Escudero, J. M., Torres-García, A. E., Gonzalo, R., & Ederra, I.(2020). A Gap Waveguide-Based Compact Rectangular Waveguide to a Packaged Microstrip Inline Transition. Applied Sciences, 10 (14), 1-13.

[7] Pérez, J. M., Rebollo, A., Gonzalo, R., & Ederra, I. (2016). An In-line Microstrip-to-waveguide Transition operating in the full W-Band based on a Chebyshev Multisection Transformer. 2016 10th European Conference on Antennas and Propagation (EuCAP), Davos, 1-4.

[8] Pérez-Escudero, J. M., Torres-García, A. E., Gonzalo, R., & Ederra, I. (2018). A Simplified Design Inline Microstrip-to-Waveguide Transition. Electronics, 7 (10), 1-11.

[9] Simone, M., Fanti, A. Valente, G., Montisci, G., Ghiani, R., & Mazzarella, G. (2018). A Compact In-line Waveguide-to-Microstrip Transition in the Q-Band for Radio Astronomy Applications," Electronics, 7, 2, 1-8.

[10] Li, C. L., Jin, C., Ma, H. Q., & Shi, X. W. (2019). An In-line Waveguide-to-Microstrip Transition for Wideband Millimeter- wave Applications," Microwave and Optical Technology Letters, 1-5.

[11] Varshney, A. K. (2013). A Microwave Rectangular Waveguide-to-Micro-strip line Transitions @ 30 GHz. International Journal of Emerging Technology and Advanced Engineering, 3 (8), 563-568.

[12] Murphy, E. R. (1984). Microstrip to waveguide transition. US Patent 4,453,142.

[13] Malik, Z.Y., Nawaz, M.I., & Kashif, M. (2010). MMIC/MIC Compatible Planar Microstrip to Waveguide Transition at Ku-Band For Radar Applications. Proceedings of International Bhurban Conference on Applied Sciences & Technology , Islamabad, Pakistan, ,11 – 14 Jan, 2010, 51-53.

[14] Li, J., Xu, J., & Fu, J. (2012). A full Ka-band Microstrip-to-Waveguide Transition Using Side-Inserted Magnetic Coupling Semicircular Ring. Proc. IEEE Wireless Microw. Technol. Conf. (WAMICON), 1-6.

[15] Shih, Y. C., Ton, T. N., & Bui, L. Q. (1988). Waveguide-to-Microstrip Transitions for mm-wave Applications. IEEE MTT-S Int. Symp. Dig., New York, 1, 473-475.

[16] Grapher, W., Hudler, B., & Menzel, W. (1994). Microstrip to Waveguide Transition Compatible with MM-wave Integrated Circuits. IEEE Trans. Microwave Theory Tech., 42, 1842-1843, 1994.

[17] Grabherr, W., & Menzel, W. (1992). A new Transition from Microstrip Line to Rectangular Waveguide. 22nd European Microwave Conference, Helsinki, Finland, 1170-1175.

[18] Villegas, F. J., Stones, D. I., & Hung, H. A. (1999). A Novel Waveguide-to- Microstrip Transition for Millimeter-wave Module Applications. IEEE Trans. Microwave Theory Tech., 47, 48-55.

[19] Tomar, S., Singh, S. K., Suthar, L., Singh, R. B., & Kumar, A. (2010). E-Plane Waveguide-to-Microstrip Transition for Wave Applications. ICMARS 2010.

[20] Van Heuven, J. H.C. (1976). A New Integrated Waveguide-Microstrip Transition. IEEE Transactions on Microwave Theory and Techniques, 24, 144 - 147, 1976.

[21] Sakakibara, K., Hirono, M., Kikuma, N. & Hirayama, H. (2008). Broadband and Planar Microstrip-to-Waveguide Transitions in mm-wave Band. International Conference on Microwave and Wave Technology, 1278-1281.

[22] guyen, B. D., Migliaccio, C., Pichot, C. & Rolland, N. (2005). Design of Microstrip to Waveguide Transition in the W-Band Suitable Antenna or Integrated Circuits Connections. Microwave and Optical Technology Letters, 47 (6), 518-520.

[23] Lin, T.H.& Wu, R.B. (2002). A Broadband Microstrip-to-Waveguide Transition with Tapered CPS Probe. 32nd European Microwave Conference, Milan, Italy, Sept 23-26, 2002, 1-4.

[24] Ijuka, H., Watanabe, T., Sato, K., & Nishikawa, K. (2002). Millimeter-wave Microstrip Line to Waveguide Transition Fabricated on a Single Layer Dielectric Substrate. Special Issue Millimeter-Wave Radar for Automotive Applications, R&D Review of Toyota, CRDL,

, 23, April, 2002, 37 (2), 13-18.

[25] Tong, Z., & Stelzer, A. (2012). A Vertical Transition between Rectangular Waveguide and Coupled Microstrip Lines. IEEE Microwave and Wireless Components Letters, May 2012, 22 (5), 251-253.

[26] Fang, R. Y., & Wang, C.-L. (2013). Miniaturized Microstrip-to-Waveguide Transition using Capacitance-Compensated Broadside-Coupled Microstrip Line. IEEE Transactions on Components, Packaging and Manufacturing Technology, Sept 2013, 3 (9), 1588-1596.

[27] Ariffin, A., Isa, D., & Malekmohammadi, A. (2016). Broadband Transition from Microstrip Line to Waveguide using a Radial Probe and Extended GND Planes for Millimeter-Wave Applications. Progress in Electromagnetics Research Letters, May 26, 2016, 60, 95-100.

[28] Meyer, A., Karau, S., & Schneider, M. (2020). Broadband Stacked-Patch Transition from Microstrip Line to Circular Dielectric Waveguide for Dual-Polarized Applications at W-Band Frequencies. 2019 49th European Microwave Conference (EuMC), Paris, France, published (online), 27, April 2020, 440-443.

[29] Gupta, R., & Kumar, P. P. (2020). Improved Design of Ka-band Waveguide to Coaxial Right Angle Microwave Transition. URSI RCRS 2020, IIT (BHU), Varanasi, India, Feb 2020, 12-14.

[30] Tang, C., Pan, X., Cheng, F., & Lin, X. (2020). A Broadband Microstrip-to-Waveguide End-wall Probe Transition and its Application in Waveguide Termination. Progress in Electromagnetics Research Letters, Jan 2020, 89, 99-104.

[31] Pozar, D. M. (2016). Microwave Engineering. Chapter-4: Microwave Network Analysis. Wiley Student edition, 4th ed., , New Delhi, India, 165-220.